

The influence of electrolyte composition on electrochemical ferrate(VI) synthesis. Part II: anodic dissolution kinetics of a steel anode rich in silicon

Zuzana Mácová · Karel Bouzek

Received: 14 March 2011 / Accepted: 5 July 2011 / Published online: 22 July 2011
© Springer Science+Business Media B.V. 2011

Abstract The anolyte composition and process temperature could improve the kinetics of iron anode dissolution and subsequent ferrate(VI) production significantly. This also holds for the anode composition. Silicon-rich steel (SRS) was employed as the anode material to produce ferrate(VI), and the characteristics observed were compared with those of the pure iron anode obtained during our previous study. Using anolytes 14 M NaOH, 14 M KOH and mixtures thereof, the systems were studied by means of potentiodynamic methods, electrochemical impedance spectroscopy and batch electrolysis experiments. In addition, scanning electron microscopy and metallographic images of the material surface were taken to identify changes in the phase composition of the material, caused by anodic polarization in strongly alkaline solutions. The dissolution kinetics increases with increasing temperature and, at 60 °C, also with increasing K⁺ content in the anolyte. Compared to iron, SRS easily dissolves into ferrate(VI), even at 20 °C in pure NaOH, indicating the lower inferior protective properties of oxy-hydroxide surface layers. The current efficiency achieved was almost 55% under these conditions. In the other anolytes, a maximum current efficiency of ca. 40% was obtained at 60 °C. The authors conclude that, at 60 °C, the efficiency is lowered by intensified oxygen evolution. This causes intensive solution convection, disturbing the surface conditions supporting ferrate(VI) formation.

Keywords Ferrate(VI) · Dissolution kinetics · Silicon content · Electrolyte composition · Electrode composition

1 Introduction

This article focuses on the electrochemical synthesis of a ferrate (ferrate means ferrate(VI) throughout this text), a compound of iron in the oxidation state +VI. Lacking six electrons in the valence shell, ferrate represents one of the strongest oxidants. Owing to its high oxidation power, it could be used in several industrial applications, especially in drinking and/or waste water treatment technology [1].

The low stability of ferrate in an aqueous environment still complicates the production of pure ferrate in sufficient amounts and at a reasonable cost. There are several ways of synthesizing ferrate, some of them have been known for more than two centuries [2]. Of these, only the electrochemical method is an easy-to-operate procedure, providing a product of high purity. A recently published review article [2] summarized the current state-of-the-art of this method, including its advantages and limitations. A following article brought the results of our first attempt to find the optimum conditions for ferrate synthesis from the point of view of the cation composition of the electrolyte and the process temperature [3]. Pure iron served as the anode in this case. This article puts forward the electrode composition as a third parameter in the search for an optimum synthesis process. Several authors have addressed this aspect of the ferrate synthesis process. Lescuras-Darrou et al. [4] showed that, when present in the anode material, silicon positively influences ferrate production. Lapicque et al. [5] then reported the mixing of KOH with a basic NaOH electrolyte to improve the performance of a silicon-rich steel (SRS) anode. Unfortunately, this study did not

Z. Mácová · K. Bouzek (✉)
Department of Inorganic Technology,
Institute of Chemical Technology Prague, Technická 5,
166 28 Prague 6, Czech Republic
e-mail: bouzeck@vscht.cz

involve an accurate adjustment of the temperature and the molar concentration of the OH^- ion. Regarding the results of these investigations [4, 5], the mechanism of the dissolution of an SRS material seems to differ from that of pure iron. In [6], it was stated that in the white cast iron anode the Fe_3C phase dissolves readily even at lower temperatures compared with the rest of the anode material. This leads to the continuous exposure of new/fresh anode material. Thus, at low temperatures (20°C) white cast iron anode dissolves faster than a pure iron one. One theory suggested here is that silicon may depress the inhibition of surface dissolution in the same way as Fe_3C . This article results from an attempt to verify this theory. In addition, the authors aimed to define the optimum conditions, i.e. temperature, current density and electrolyte composition, for ferrate synthesis with an SRS anode.

The potentiodynamic voltammetric (PV) experiments, electrochemical impedance spectroscopy (EIS) measurements and batch electrolyses enabled us to interpret the dissolution mechanism of SRS. The investigations were conducted in electrolytes similar to those identified in [3], and similar conditions were applied. This made it possible to compare the characteristics obtained with SRS and pure iron. Furthermore, SEM images and metallographic analysis were used to detect changes in the surface state.

The kinetics of the electrochemical step in the ferrate formation mechanism is faster when SRS is employed as the anode. This anode already dissolves readily at 20°C with sufficient current efficiency compared with iron which showed a partial inhibition of the surface. The metallographic analysis and SEM images prove that the presence of silicon inclusions in the SRS structure significantly reduces inhibition of the surface.

2 Experimental

A detailed description of the chemicals, apparatus and procedures used can be found in [3]. The following information is supplementary. The PV and EIS experiments were performed in a classical three-electrode arrangement. The working electrode had an active surface of 0.196 cm^2 and contained 3.17 wt% Si and the following impurities: 0.47 wt% Cu, 0.23 wt% Mn and 0.03 wt% Ni (AISI M-27). The results are related to an HgO/Hg reference electrode with 14 M NaOH as the internal electrolyte. The counter-electrode was a platinum plate with an active surface area of 0.84 cm^2 . The working electrode was cathodically pre-polarized at 20 mA cm^{-2} for 5 min before each experiment. In the case of the PV experiments, a recording of the polarization curve at the studied sweep rate ($5\text{--}500\text{ mVs}^{-1}$) immediately followed pre-polarization. In the case of the EIS experiments, the electrode

potential was held at a required value for 10 min, and then an impedance spectrum was recorded in the frequency range of 60 kHz – 10 mHz . An *ac* signal amplitude of 10 mV was used. All the experiments were performed under nitrogen atmosphere.

The batch electrolyses were carried out in galvanostatic mode in a cell with a PVC diaphragm separating the anode and cathode compartments. The active surface area of the anode was 51.6 cm^2 , the anolyte volume comprised 70 cm^3 . The galvanostatic experiment was carried out for 180 min after 30 min cathodic pre-polarization at 20 mA cm^{-2} .

Before a metallographic analysis, the sample of anode material was polished with P4000 emery paper (Buehler, USA). The sample was then etched in a 2% HNO_3 solution in ethanol for approximately 2 min at room temperature.

Before SEM analysis, the following procedure was applied: the electrode surface was cathodically pre-polarized at a current density of 20 mA cm^{-2} for 5 min. The polarization was then immediately switched to anodic and a current density of 15 mA cm^{-2} was applied for 15 min. After polarization, the electrode was rinsed with distilled water, dried in hot air and analysed immediately. During this SEM study, 14 M KOH or 14 M NaOH was used as electrolyte at temperatures of 20 or 60°C .

3 Results and discussion

3.1 Voltammetric experiments

The current peaks observed on the polarization curve of SRS in the two electrolyte solutions at 20°C (Fig. 1) can be ascribed to reactions similar to those for an iron electrode in [3]

Peak AI: oxidation of metallic Fe to $\text{Fe}(\text{II})$, Eq. 1 in [3]

Peak AII: oxidation of $\text{Fe}(\text{II})$ to $\text{Fe}(\text{III})$, Eq. 2A–2C in [3]

Peak AIII: the restructuring of the anode surface layer

Peak AIV: reactions related to ferrate formation, Eq. 6 in [3]

Peak CIII: ferrate reduction to $\text{Fe}(\text{III})$

Peak CII: reduction of the surface layer from $\text{Fe}(\text{III})$ back to $\text{Fe}(\text{II})$

Peak CI: subsequent reduction to $\text{Fe}(0)$

Compared to the iron electrode, several differences were observed. Firstly, the current density increased in the passivity region (-0.1 to 0.48 V at 20°C , NaOH), forming a new current density peak AIIIB. With increasing temperature, this peak was shifted to more cathodic potentials. Secondly, new peaks were found in the potential region of cathodic reduction ($\leq 0.65\text{ V}$). In both the cases, the new peaks are most probably related to the phase structure change of the SRS electrode.

Comparing the polarization curves for the individual electrolytes in Fig. 1, KOH showed a higher current density at 20 °C. However, increasing temperature also resulted in a significant increase in current density in NaOH, especially in the potential region of the AlIIB peak.

On all polarization curves, a significant hysteresis was observed in the region of anodic switch potential. This should be attributed to a considerable diminution in the inhibition of the electrode surface most probably caused by intensive oxygen evolution.

The higher current density response in KOH in the potential region of peaks CI–CIII can be explained by the higher amount of reducible products, mainly ferrate, deposited on the electrode surface under the experimental conditions. Owing to the relatively low current density values in the potential region of –0.1 to 0.4 V in the reverse sweep, it is possible that these products are deposited in solid form.

The subsequent addition of K⁺ ion to the basic NaOH electrolyte (not documented here) caused a gradual potential shift of both the initiation of the transpassive region (peak AIV) and the peak CIII position to more cathodic values. This proves the gradual passivation of the electrode surface towards the chemical dissolution in the potential region of –0.4 to 0.2 V. The gradual increase in current

density of peak CIII may be ascribed to the higher amount of solid product depositing on the electrode surface.

An analysis of the Tafel slope of pseudo-stationary polarization curves taken at a potential sweep rate of 5 mV s⁻¹ is in good agreement with the iron electrode results [3]. This corresponds to the theory that the electrochemical reaction connected with the current density increase in the potential region of peak AIV is due to a one-electron transition. This indicates that the material itself does not influence the mechanism of ferrate formation.

The influence of the potential sweep rate on the characteristics of peaks AIV and CIII was studied in the next step. The current density value at a potential corresponding to peak AIV increased with the potential sweep rate under all conditions being studied (electrolyte composition; temperature) (Fig. 2). However, after reaching a certain maximum at ca. 100–200 mV s⁻¹, the increasing potential sweep rate led to a decrease in current density. This might be associated with a chemical step preceding the electrochemical one in the reaction mechanism [3]. The chemical step seems to become rate determining when the potential sweep rate exceeds ca. 100 mV s⁻¹.

The current density values increased with increasing temperature, thus documenting an enhancement of the electrochemical reaction kinetics. At the same time, the

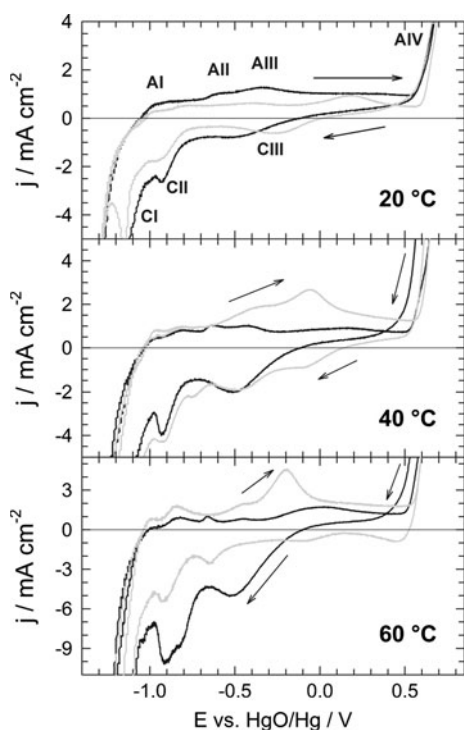


Fig. 1 The polarization curves of the SRS electrode in NaOH (black) and KOH (grey) at a potential sweep rate of 5 mVs⁻¹. The temperature is indicated on the graphs; arrows indicate the sweep direction

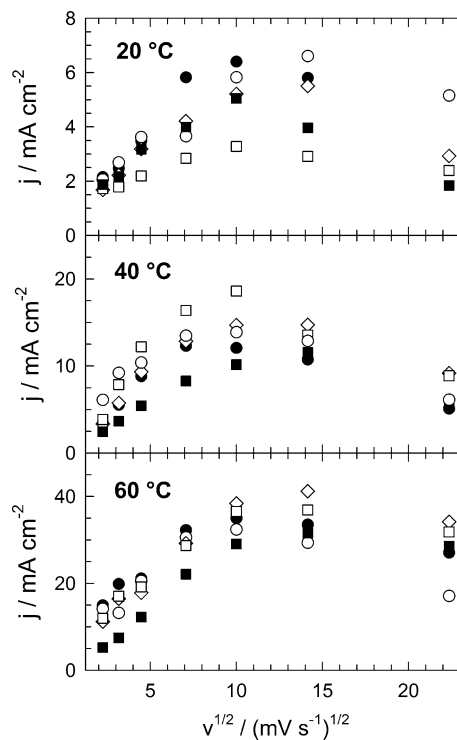


Fig. 2 The dependence of the current density in the potential region of peak AIV on the potential sweep rate. Electrolyte composition: filled circle NaOH, open circle Na⁺:K⁺ = 3:1, rhombus Na⁺:K⁺ = 1:1, open square Na⁺:K⁺ = 1:3, filled square KOH; the temperature is indicated

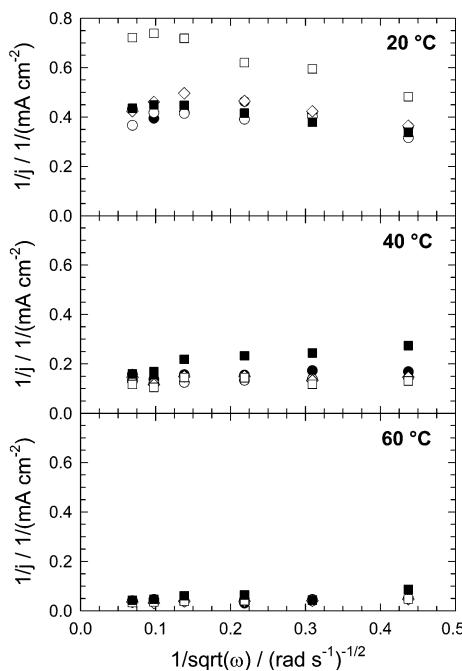


Fig. 3 The dependence of the reciprocal value of the current density read at one potential in the peak AIV potential region on square root of the rotational speed. Electrode: SRS; electrolyte composition: filled circle NaOH, open circle $\text{Na}^+:\text{K}^+ = 3:1$, rhombus $\text{Na}^+:\text{K}^+ = 1:1$, open square $\text{Na}^+:\text{K}^+ = 1:3$, filled square KOH; the temperature is indicated in the graphs

role of the individual cations (K^+ and Na^+) in the product formation mechanism obviously changed. At 20 °C, the highest current density was attained in NaOH. At 60 °C, it was similarly high for all mixed solutions and NaOH. This was caused by the changing the solubility of the reaction intermediates and products.

The current density value of peak CIII increased with increasing potential sweep rate in the entire temperature range being studied (not shown here). This increase corresponds to the diffusion of the ferrate product originating at the electrode (at the potential of peak AIV) from the surface to the bulk of the electrolyte. The increase is not so steep for electrolytes with a high K^+ content, again documenting the effect of changing ferrate solubility. The current density of peak CIII also increased with increasing temperature. In NaOH at 60 °C, however, ferrate reduction is observed only at a high potential sweep rate, since the

product decomposes rapidly under these conditions. In comparison with the pure iron electrode [3], the current density of CIII was higher in the case of the SRS electrode.

In the next step, the influence of mass transport on the system behaviour was studied by means of a rotating disc electrode. The polarization curve changed only slightly with an increasing electrode rotation rate. Firstly, the current density values increased in the passivity potential region. This indicates that the process taking place in the passivity region depends on the mass transport to or from the electrode surface. In agreement with Zou and Chin [7], it can be concluded that in this potential range the electrode dissolution products precipitate on the electrode surface in the form of a salt layer. Secondly, the current density of peaks AIV (Fig. 3) and CIII decreased with increasing electrode rotation rate. This corresponds to the fact that the reactants and products were drawn away from the electrode vicinity and, therefore, could not participate in the electrode processes. Thirdly, the hysteresis of the polarization curves in the transpassive potential region was more pronounced at a higher rotation speed. This constitutes evidence of lower electrode passivation due to higher electrolyte convection. It leads to the intensive transport of precipitating salts to the electrolyte bulk, and more intensive oxygen evolution.

The data from Fig. 3 were processed by Koutecky-Levich analysis, the method being described in detail in [3], and the values of kinetic current density were calculated (Table 1).

The data in Table 1 show that temperature is essential to the increase in electrode reaction kinetics in all the anolyte solutions studied. The presence of a second cation (K^+) in the electrolyte exhibited a positive influence at elevated temperatures, since the highest values of kinetic current density were observed in all mixed solutions at 40 and 60 °C.

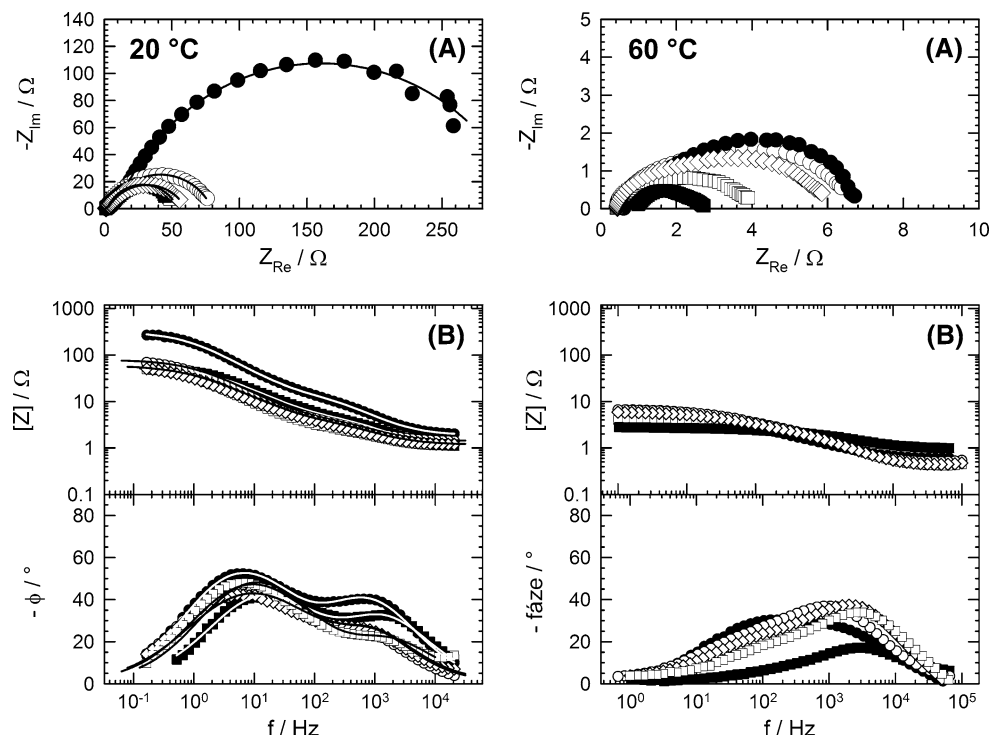
3.2 EIS experiments

An example of the impedance spectra obtained for the SRS electrode is given in Fig. 4. Similar to the iron electrode [3, 8], the process exhibits two kinetic constants at the SRS electrode. Therefore, the physical model of two macro homogeneous surface layers was applied in this case, too.

Table 1 The values of kinetic current density (mA cm^{-2}) of the SRS electrode at the temperatures studied in 14 M OH^- solutions of various $\text{Na}^+:\text{K}^+$ ratios

Solution	°C	NaOH	$\text{Na}^+:\text{K}^+ = 3:1$	$\text{Na}^+:\text{K}^+ = 1:1$	$\text{Na}^+:\text{K}^+ = 1:3$	KOH
j_K	20	2.3 ± 0.2	2.2 ± 0.3	1.9 ± 0.2	1.3 ± 0.3	2.0 ± 0.3
	40	7.2 ± 0.5	8.3 ± 0.5	6.7 ± 0.7	8.3 ± 0.9	6.5 ± 1.0
	60	27.7 ± 3.8	29.1 ± 2.2	29.9 ± 3.2	30.6 ± 3.0	25.8 ± 4.4

Fig. 4 The EIS spectra of SRS in the electrolytes studied at 20 °C (on the right) and at 60 °C (on the left). The spectra are shown in Nyquist (**a**) and Bode (**b**) plots. Full lines represent data calculated from the theoretical model [3]. Potential: 600 mV; electrolyte composition: filled circle NaOH, open circle $\text{Na}^+:\text{K}^+ = 3:1$, rhombus $\text{Na}^+:\text{K}^+ = 1:1$, open square $\text{Na}^+:\text{K}^+ = 1:3$, filled square KOH



The theory of the duplex sandwich assembly of the passivating layers was taken into account similarly as was done in [9], and similar to that article the “passive pit” model [10] was then used for data processing. An equivalent circuit expressing this model consists of two parallel R-CPE elements and one resistance element connected in series (see Fig. 5 in [3] for a detailed description). The solid lines in Fig. 4a represent the data calculated on the

basis of an equivalent circuit using the parameters optimized from the experimental data. They also confirm that the proposed model agrees well with the experimental data.

The optimized parameters were further processed, as shown, for example, in Fig. 5 for NaOH. The resistance values of the inner layer were approximately constant up to an electrode potential of 500 mV, and slowly decreased with a further increase in potential. The resistance of the

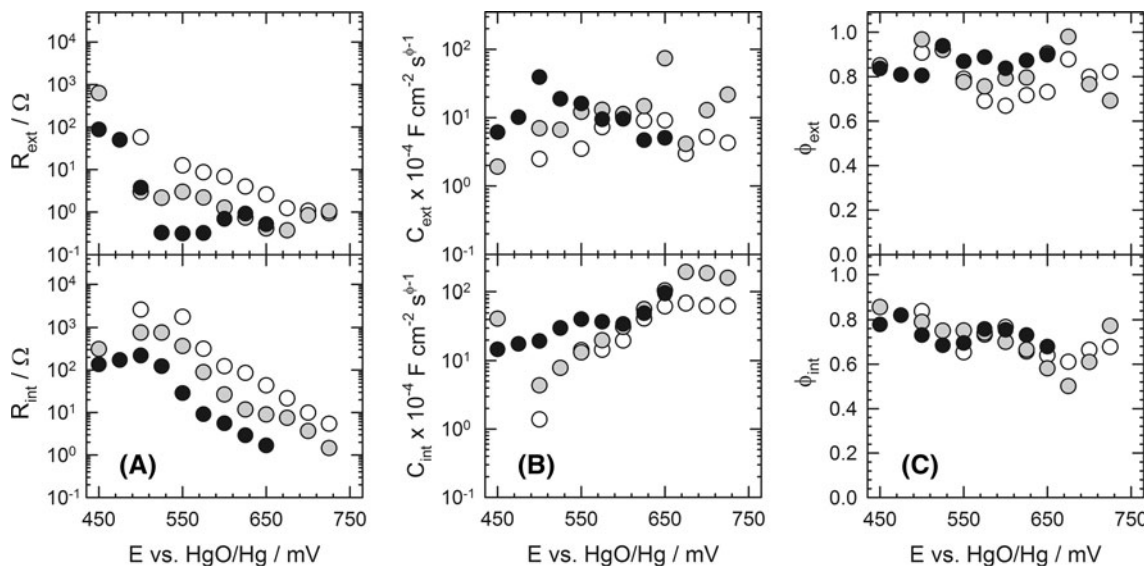


Fig. 5 The fitted values of the equivalent circuit elements: resistance (**a**), capacitance (**b**) and parameter ϕ (**c**) obtained for the layers in dependence on the anodic polarization potential of the SRS electrode

in pure NaOH electrolyte at various temperatures: 20 °C white, 40 °C grey, and 60 °C black symbols

outer layer continuously decreased with increasing potential at 20 and 40 °C. At 60 °C, this resistance dropped drastically to almost zero at 525 mV and remained constant at higher potential values. This indicates the total disappearance of the layer from the electrode surface. The increasing temperature caused a gradual decrease in the resistance of both the inner and the outer layer.

The two-layer capacities increased with temperature. The inner-layer capacity, C , increased with applied potential up to a certain limit (675 mV at 20 and 40 °C; 550 mV at 60 °C), and then remained almost constant. This indicates a decrease in the thickness of the inner layer or an increase in real surface, and thus its protective capacity gradually declined. This is further documented by a gradual decrease in the parameter ϕ . The capacity of the outer layer also increased slightly with the applied potential, indicating its increasing porosity. Its values, however, became very scattered (which also holds for the parameter, ϕ). It can be assumed that the outer layer disintegrates at a high temperature and potential and does not represent a significant barrier for the electrochemical reactions to take place at the electrode surface.

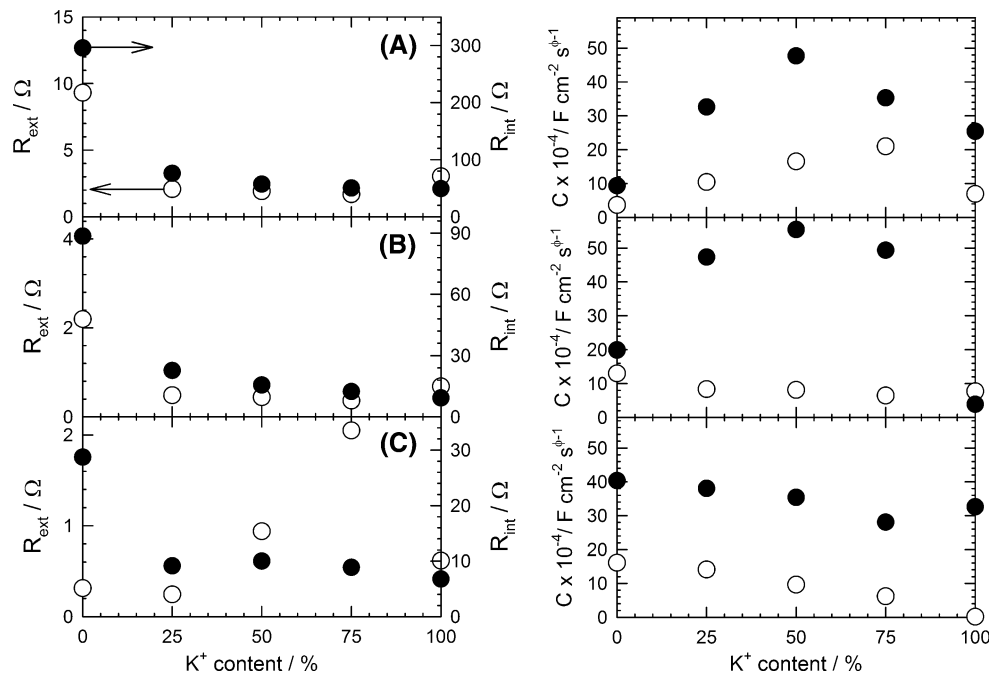
A comparison of the fitted values for the individual electrolytes (Fig. 6) shows dependencies on the increasing K^+ content similar to the iron electrode [3]. The inner-layer resistance decreased dramatically with the first addition of K^+ to a basic NaOH solution and then remained almost constant. At temperatures of 20 and 40 °C (denoted as (a) and (b) in Fig. 6, respectively), a similar drop was observed in the resistance of the outer layer. At 60 °C

(denoted as (c) in Fig. 6), the resistance of the outer layer gradually increased with the K^+ content up to a ratio of $Na^+ : K^+ = 1:3$ and again dropped significantly in KOH.

The maximum capacitance of the inner layer was achieved in the solution $Na^+ : K^+ = 1:1$ at 20 and 40 °C. At 60 °C, the capacitance gradually decreased with increasing K^+ content. The resistance of the outer layer progressively increased with K^+ content up to a solution composition of $Na^+ : K^+ = 1:3$ at 20 °C. By contrast, its values continuously decreased at a higher temperature.

Comparing the behaviour observed for the iron electrode, the layers covering the SRS electrode surface are less stable. The outer layer lost its protective properties entirely (a resistance value lower than 1 Ω) under far milder conditions than in the case of pure iron. The inner layer also became porous at a high temperature and potential, and its resistance dropped to units of Ohms. The drop in the resistance of the layers was generally further accentuated by the presence of K^+ in the solution. On the other hand, this most probably led to marked stabilization in the case of the outer layer as the parameter C decreased with increasing content of K^+ . Here, two counteracting factors should be considered. On the one hand, the more aggressive character of the electrolyte with higher K^+ content causes intensive layer disintegration. On the other hand, the lower solubility of the dissolution products (K_2FeO_4 or potassium salts of the intermediate products) leads to their precipitation into the pores of the outer layer, causing the subsequent stabilization of the layer.

Fig. 6 The fitted values of resistance (left) and capacitance (right) values obtained for the outer (circle) and inner (filled circle) layers at a potential of 600 mV at 20 °C (a), 575 mV at 40 °C (b) and 550 mV at 60 °C (c) in dependence on electrolyte composition, i.e. K^+ ion content in the 14 M OH^- solution



3.3 Batch electrolyses

The current efficiency of the batch electrolyses was calculated with respect to the ferrate concentration in the anolyte, resulting from 3-hours electrolysis (Fig. 7). At 20 °C, the highest current efficiency of about 53% was achieved with NaOH as the electrolyte. The mixed electrolytes showed higher current efficiency (by 10–15%) than pure KOH. This documents the positive effect of the addition of Na^+ ion to enhance electrode dissolution. With a temperature increase, the current efficiency gradually decreased in NaOH. At 40 °C, the maximum efficiency values of around 35% were achieved with a solution of $\text{Na}^+:\text{K}^+ = 3:1$, but the efficiency values were well comparable in all the solutions used.

In general, the efficiency decreased with increasing current density at temperatures of 20 and 40 °C. However, this is not the case with a temperature of 60 °C, where the efficiency is nearly constant for the solutions KOH, $\text{Na}^+:\text{K}^+ = 1:3$ and $\text{Na}^+:\text{K}^+ = 1:1$ (around 35%) even at high current density.

Similar to the pure iron study [3], the current efficiency gradually decreased with temperature, when using the NaOH electrolyte. Rapid product decomposition is responsible for the efficiency decrease in NaOH in the case of the pure iron

electrode. In the case of the SRS electrode, another process affects the current efficiency value at higher temperatures. The data in Fig. 8 describe how the iron content in oxidation states lower than +VI in the solution developed with increasing current density. At 20 °C, the current efficiency is reduced by the product decomposition in NaOH. Yet, the low current efficiency is caused by the parasitic reaction of oxygen evolution, rather than ferrate decomposition at higher temperatures. This follows from the concentration dependency of iron in an oxidation state lower than VI+ in the solution, which does not increase substantially with current density. Ferrate decomposition caused lower efficiency only in $\text{Na}^+:\text{K}^+ = 3:1$ solution at 60 °C. The use of other solutions led to a more stable product.

The results reveal that the kinetics of individual reactions has a significant effect on the dissolution of the material. The composition of the anode material is mainly essential for fast dissolution at low temperatures, at which the dissolution of pure iron is very slow. This statement is especially valid for NaOH as an anolyte. The solubility of the product in solutions containing K^+ is low, and therefore, it leads to a surface blockage to further dissolution. At higher temperatures, the dissolution yielded to oxygen evolution in NaOH. In the other solutions, the stability of the product was still sufficient; the arising solid salts of

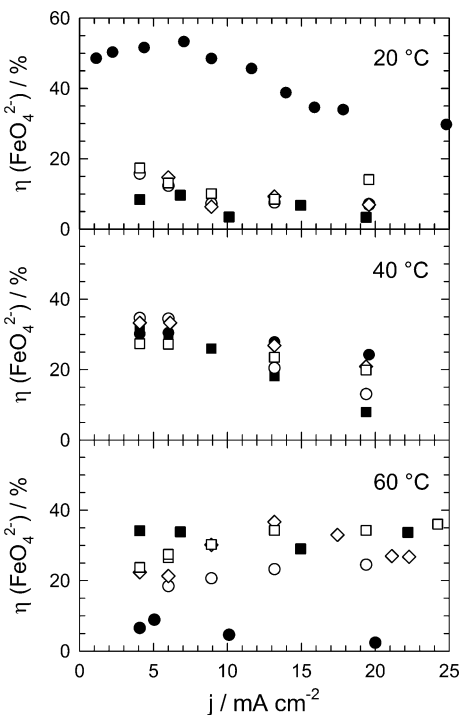


Fig. 7 Dependence of current efficiency of ferrate formation after 180 min of batch electrolysis on anodic current density at various temperatures obtained for the individual electrolytes used: filled circle NaOH, filled square KOH, open circle $\text{Na}^+:\text{K}^+ = 3:1$, rhombus $\text{Na}^+:\text{K}^+ = 1:1$, open square $\text{Na}^+:\text{K}^+ = 1:3$; electrodes: SRS

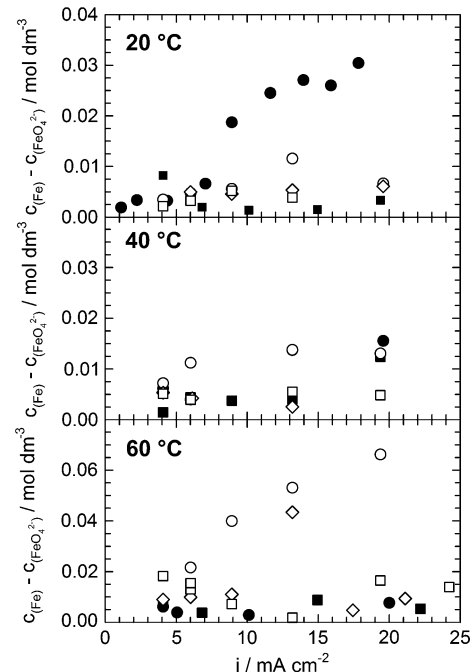


Fig. 8 Dependence of the difference in molar concentration of the total iron and FeO_4^{2-} contained in the electrolyte on completion of electrolysis on the anodic current density applied at various temperatures for the individual electrolytes under study: filled circle NaOH, filled square KOH, open circle $\text{Na}^+:\text{K}^+ = 3:1$, rhombus $\text{Na}^+:\text{K}^+ = 1:1$, open square $\text{Na}^+:\text{K}^+ = 1:3$; electrodes: SRS

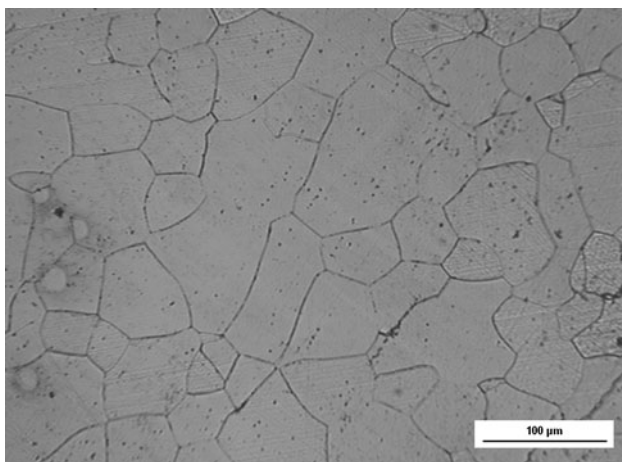


Fig. 9 Metallography of SRS after etching in 2% nital for 5 min

product did not block the electrode surface to such an extent.

On the basis of the batch electrolysis results, the most efficient process conditions were determined to be NaOH solution at 20 °C at a current density of approximately 5 mA cm⁻². Other conditions could be recommended for the industrial application of electrochemical ferrate synthesis: at 60 °C, the synthesis could be operated at high current densities (up to 30 mA cm⁻²) without loss of efficiency due to ferrate decomposition.

3.4 Metallography and SEM analysis

A metallographic image of the SRS material is shown in Fig. 9. The material is constituted of individual grains of ferrite with homogeneously dissolved silicon; the silicate inclusions originating from steel production are confirmed by well-detectable black dots on the material surface.

The SEM images of the SRS anode surface taken after 15 min of polarization at 20 °C are given in Fig. 10.

In NaOH, SRS dissolves most intensively at the grain boundaries; thus the porosity of the material increases. The segregated silicon most probably accumulates at the grain boundaries where it induces anodic dissolution. It was also observed that the dissolution proceeded intensively in the surface area of the silicate inclusions (Fig. 10, on the left). This supports the theory of limitation of the electrode surface, caused by the passivity of the electrode surface due to silicon dissolution from its structure. The dissolution is then less selective in KOH. Compared with NaOH, the silicate inclusions seemed to be inert towards the dissolution in KOH. This finding is in agreement both with the voltammetry and the batch experiment results. While the voltammetric experiments showed the anodic peak in the transpassivity potential region corresponding to the exposure of the fresh electrode surface, the batch electrolyses showed the highest efficiency under these conditions.

The SEM images of SRS, taken after polarization at 60 °C, show more intensive dissolution of the material in both electrolytes (Fig. 11). A detailed analysis of these photographs is complicated by the fact that the bare surface of the material is not visible. It could be assumed that the mode of dissolution is the same as at 20 °C. In the case of dissolution in NaOH solution, the surface is covered by a strongly hydrated layer that flaked from the surface after drying (see Fig. 11 on the left). In the electrolytes containing K⁺, the surface irregularities indicate that the silicate inclusions probably fall out of the material as a whole during dissolution and reveal the new electrode surface for the electrolytic action. This promotes the continuous activation of the electrode surface.

4 Conclusion

The SRS material was found to be a suitable anode material for electrochemical ferrate synthesis. The surface of an iron

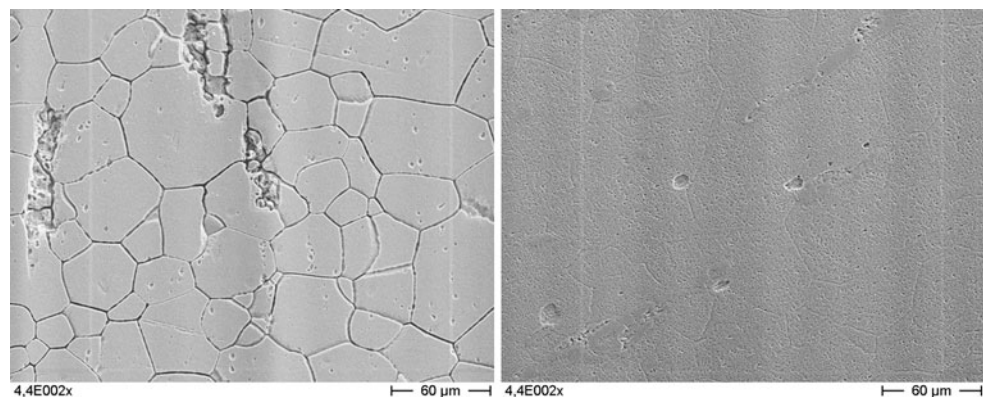


Fig. 10 SEM images of SRS after 15 min anodic polarization at 20 mA cm⁻² in NaOH (on the left) and KOH (on the right), temperature 20 °C

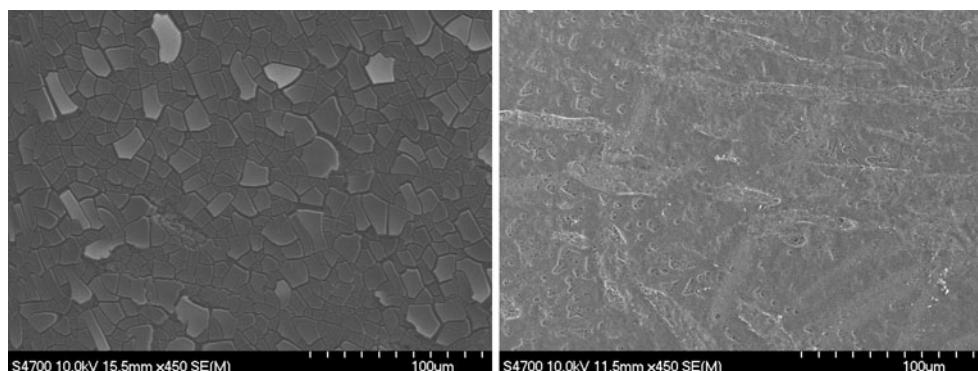


Fig. 11 SEM images of SRS after 15 min anodic polarization at 20 mA cm^{-2} in NaOH (on the left) and KOH (on the right), temperature 60°C

material alloyed with silicon dissolves rapidly even at 20°C in pure NaOH. This is caused by less protective surface layers and by favorable dissolution of the silicate phase from the material's structure. Since the solubility of ferrate is lower in solutions containing K^+ , KOH and mixed solutions are preferred as anolytes at higher temperatures because the ferrate formed is stabilized in a solid form. At 60°C , the ferrate formation process is disrupted by intensive oxygen evolution. However, using the SRS anode, the authors did not observe the inhibition that is usual for a pure iron anode at high current density.

The authors therefore conclude that the most efficient process conditions appear to be NaOH solution at 20°C and a current density value of 5 mA cm^{-2} .

Acknowledgments The authors gratefully acknowledge the financial support of this research by the Ministry of Education, Youth and Sports within projects Nos. ME890 and MSM6046137301. The

authors would also like to express their thanks to Ing. Zuzana Cílová, Ph.D. for the SEM images and the analysis thereof.

References

1. Sharma VK (2002) *Adv Environ Res* 6:143
2. Macova Z, Bouzek K, Hives J et al (2009) *Electrochim Acta* 54:2673
3. Macova Z, Bouzek K, Sharma VK (2010) *J Appl Electrochem* 40:1019
4. Lescuras-Darrou V, Lapicque F, Valentin G (2002) *J Appl Electrochem* 32:57
5. Lapicque F, Valentin G (2002) *Electrochim Commun* 4:764
6. Bouzek K, Roušar I, Taylor MA (1996) *J Appl Electrochem* 26:925
7. Zou J-Y, Chin D-T (1988) *Electrochim Acta* 33:477
8. Híveš J, Máková Z, Benová M et al (2008) *J Electrochem Soc* 155:E113
9. Bouzek K, Bergmann H (1999) *Corros Sci* 41:2113
10. Jüttner K (1990) *Electrochim Acta* 35:1501